2010 IEEE International Conference on Robotics and Automation
Anchorage Convention District
May 3-8, 2010, Anchorage, Alaska, USA

# Planar Path Planning for Flight Vehicles in Wind with Turn Rate and Acceleration Bounds

Laszlo Techy*, Craig A. Woolsey† and Kristi A. Morgansen‡

*Abstract*— **This paper is concerned with path planning for an autonomous flight vehicle operating in a steady, uniform flow-field. We model the vehicle as a particle that travels in the horizontal plane at a constant speed relative to the ambient flow. The vehicle may turn in either direction, subject to symmetric constraints on the turn rate and the turn acceleration. The contribution of the paper is a simple method for generating candidate minimum-time paths from a given initial point and heading to a given final point and heading.**

## I. Introduction

A variety of civilian and scientific applications for autonomous vehicles are being pursued, including mining [1], search and rescue [2], and surveillance and reconnaissance [3]. Applications that are envisioned for the future will place increasingly stringent demands on vehicle performance. Autonomous flight vehicle applications, for example, may require effective operation in confined or cluttered domains and/or in significant winds. Commercial autopilots can be readily integrated into modern flight vehicles and can easily accomplish low-level control tasks, such as maintaining straight-and-level or turning flight. Higher level guidance algorithms provide turn rate inputs for the low-level control loops to achieve convergence to desired paths, typically sequences of straight segments connecting user-specified waypoints. Because a flight vehicle cannot instantaneously change course, the guidance algorithm may incorporate some transient maneuver (a "pre-turn," for example) to transition smoothly between straight segments. This approach to path planning and guidance does not account, however, for the effect of ambient wind or for the limitations on turn rate and turn acceleration.

Here we consider the problem of designing a path that connects a given initial state (position and heading) to a given final state in the same horizontal plane. The procedure is informed by prior analysis of minimum time paths for constant-speed vehicles or, equivalently, minimum length paths. The assumption of a steady, uniform flow-field makes the algorithm suitable for unmanned aerial vehicles (UAVs) flying in winds, as well as for underwater vehicles — such as underwater gliders — operating in ocean currents and unmanned surface vehicles operating in riverine environments, provided the flow-field varies slowly relative to the vehicle motion. To ensure that following the path is feasible, we require the path to be continuous, and also that the curvature is a continuous function of the path parameter.

Dubins [4] studied minimum length paths with a bound on the average curvature and proved that they may be composed only of straight segments and circular arcs. Moreover, minimum length paths comprise at most three such segments. The problem was later re-formulated and studied using Pontryagin's minimum principle in [5], and additional necessary conditions for optimality were provided in [6].

More recently, the method was applied to a UAV with a bounded turning rate flying in a steady, uniform wind [7]. In that paper, minimum-time paths are designed in the air relative frame: an inertial frame that translates with the ambient flow. The desired final point in inertial space corresponds to a point in the air relative frame, a "virtual target," that moves with the same speed as the wind and in the opposite direction. The method requires iterative solution of the Dubins problem in the air relative frame, until the interception error converges to zero. It was later established that there exists a unique solution for almost every pair of initial and final states (Theorem 3 in [8]).

An alternative solution to the path planning problem is presented in the papers [9], [10], where analytical solutions are found for a subset of candidate extremals, exploiting the geometry of the problem, and recognizing that maximum effort ("bang") turns in the air relative frame correspond to *trochoidal* curves in the inertial frame [11]. The path planning method yields trajectories that are composed of straight lines and trochoidal segments. The transition points where these segments are smoothly joined together, however, correspond to points where the path curvature is discontinuous. At these points the vehicles would need to change the turn rate instantaneously. While this is possible for some

*Research Associate, Department of Aeronautics and Astronautics, University of Washington, techy@u.washington.edu, IEEE Member.

†Associate Professor, Department of Aerospace and Ocean Engineering, Virginia Tech, cwoolsey@vt.edu, IEEE Senior Member.

‡Associate Professor, Department of Aeronautics and Astronautics, University of Washington, morgansen@aa.washington.edu, IEEE Senior Member.

mobile robots, it is not feasible for fixed-wing flight vehicles.

Continuous-curvature path planning was studied in [12]. It was shown that extremal paths contain *clothoidal* curves, i.e. curves which have linearly varying curvature, and straight segments. Later it was shown that these extremal paths may be composed, in general, of an infinite number of pieces [13]. In [14], a simple path planning method is presented that exploits the geometrical symmetry of the optimal paths. The solutions can be found analytically, and they may be composed of clothoids, circular arcs, and straight segments, generalizing Dubins paths to the case where turn acceleration bounds are present. Because of the anticipated complexity of finding all extremal solutions, the search for optimal trajectories is confined to a finite set. The proposed paths are referred to as *Simple Continuous-Curvature* (SCC) paths. The algorithm essentially finds the points where the clothoids, circular arcs, and straight paths may be smoothly joined together, forming a feasible, continuous-curvature path. The difficulty of working with clothoid curves, for which no explicit analytical expression exists, is relaxed by the observation that the resulting paths are symmetric with respect to a characteristic line. Finding the points, where clothoid curves, circles, and straight lines may be smoothly stitched together, has been extensively studied in the past in the context of highway engineering [15], [16], and computer graphics [17]. Clothoid curves have the property that the curvature changes linearly along the path, and so does the lateral acceleration experienced by a car or train traveling along such a curve. In highway engineering, such curves are often referred to as *transition spirals* [18].

| Turn Constraint | No Wind | Uniform Wind |
|---|---|---|
| None | Straight line | Zermelo's problem[a] |
| Rate | Dubins path [4] | Convected Dubins path [9] [10] |
| Rate and Acceleration | Continuous-Curvature Dubins [19] [14] | Continuous-Curvature Convected Dubins (present work) |

[a]Zermelo's problem also addresses the case where the external flow is not uniform.

TABLE I
PATH PLANNING PROBLEMS FOR PLANAR KINEMATIC VEHICLES.

Table I summarizes the path planning problem types in the absence or presence of ambient winds, and with different control bounds. The complexity of the problem increases from the top left to the bottom right. The simplest situation is when there are no bounds on the turn rate, that is, the desired heading/course can be immediately achieved. In the absence of flow this corresponds to a straight line between initial and final points. This result is a special case of Zermelo's problem, which concerns optimal paths in flows. If there are bounds on the maximum achievable turn rate, the problem is referred to as Dubins' problem, as discussed earlier; its generalization to the case where winds are present is discussed in [10].

In this paper we present a method to find continuous-curvature paths in the presence of a steady, uniform flow-field. Similar to the work described in [14], we only consider a finite subset of all candidate extremals. We focus our attention on the candidate extremals, which are composed of an initial turn, followed by a straight segment, then followed by a second turn. The turns are composed of either three or two sub-segments. In the first case, the first sub-segment is a maximum acceleration turn, until the maximum allowed turn rate is reached. The second sub-segment is a maximum rate turn. The third sub-segment is a maximum deceleration turn, until the zero turn rate condition is reached. In the second case the maximum turn rate is not reached. Hence the intermediate (maximum turn-rate) sub-segment vanishes. Our approach focuses on identifying those switching points, where the straight segments, maximum acceleration turns, and maximum turn-rate turns can be stitched together to form a smooth, continuous-curvature path. More specifically, we use the continuity equations at the switching points (the velocity vector must be continuous) to set up a numerical root-finding problem to find the path parameter values where such transitions occur.

The paper is organized as follows. In Section II we present the vehicle model used for path planning. In Section III we present the path planning algorithm that is the main contribution of the paper. Section IV shows simulation results, and Section V provides conclusions.

## II. VEHICLE MODEL

We use a simple particle model for the UAV, described by the equations

$$\dot{x}(t) = V_a \cos\psi(t) + V_w \quad (1)$$
$$\dot{y}(t) = V_a \sin\psi(t) \quad (2)$$
$$\dot{\psi}(t) = \alpha\phi(t) \quad (3)$$
$$\dot{\phi}(t) = u(t). \quad (4)$$

Here $[x(t), y(t)]^T$ denotes the inertial position of the aircraft in the horizontal plane, $\psi(t)$ is the heading angle measured from the $x$-axis, $V_a$ is the constant airspeed, and $V_w$ is the constant wind speed, which we assume to be aligned with the inertial $x$-axis, without loss of generality. We assume that $V_w < V_a$ to ensure a feasible solution exists for arbitrary initial and final

conditions. (If $V_w \geq V_a$, some regions of state space are unreachable; see Lemma 3.2.1 in [20].)

The model described by equations (1)-(4) was selected to capture the fact that the turn rate of the vehicle cannot change instantaneously. In equilibrium turning flight, the heading rate of change can be expressed as a function of bank angle $\phi(t)$, as

$$\dot{\psi}(t) = \frac{g}{V_a} \tan \phi(t).$$

In typical aircraft operations, where the bank angle is small ($\phi(t) < 30°$), we can approximate the above relationship with the simple expression $\dot{\psi}(t) \approx g/V_a \phi(t) = \alpha\phi(t)$. Hence in equations (1)-(4) one can identify $\phi(t)$ with the aircraft bank angle. The rate of the bank angle is the control input. The aircraft lateral dynamics are primarily affected by the ailerons, which are differentially operated control surfaces on the wings. A small deflection of the ailerons results in a torque about the aircraft longitudinal axis, and ultimately an angular acceleration about the same axis. In addition to the limitations imposed by the aircraft dynamics and actuator limits, the rate of the bank angle is also constrained by structural load limits on the wings. The control signal is thus constrained to a compact set $u \in [-\bar{u}, \bar{u}]$.

Anticipating bang-bang and singular solutions, we constrain the control signal to the set $u \in \{-\bar{u}, 0, \bar{u}\}$. For a turning segment of a given sense, there are two cases to consider. In both cases, we denote by $\bar{t}$ the total time required to complete the given turn segment.

*Case 1: The maximum bank angle is reached.* In this case the turn rate is saturated, and the aircraft will continue its maximum constant rate turn for a certain time. After that, the bank angle is decreased until the aircraft reaches straight and level flight again. The turn is initiated by a maximum bank angle rate turn:

$$\phi(t) = \bar{u}t.$$

The maximum bank angle is reached at time $t_1 = \bar{\phi}/\bar{u} > 0$. The bank angle for the entire turn can be written as

$$\phi(t) = \begin{cases} \bar{u}t, & t \in [0, t_1] \\ \bar{u}t_1, & t \in [t_1, \bar{t} - t_1] \\ -\bar{u}(t - \bar{t}), & t \in [\bar{t} - t_1, \bar{t}]. \end{cases} \quad (5)$$

The heading angle is then

$$\psi(t) = \begin{cases} \alpha\bar{u}\frac{t^2}{2} + \psi_0, & t \in [0, t_1] \\ \alpha\bar{u}t_1 t + \psi_0 + C_1, & t \in [t_1, \bar{t} - t_1] \\ \alpha\bar{u}(t\bar{t} - \frac{t^2}{2}) + \psi_0 + C_2, & t \in [\bar{t} - t_1, \bar{t}]. \end{cases} \quad (6)$$

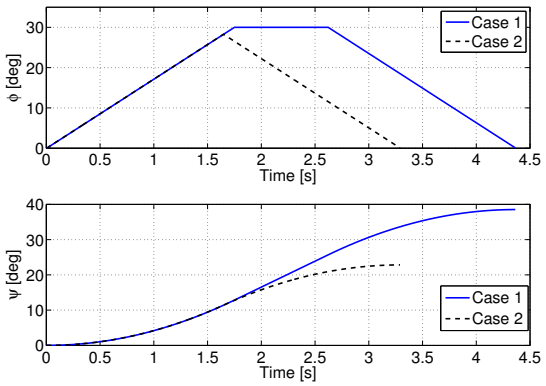


Fig. 1. Bank angle and heading angle for two different cases of turns. In *Case 1* the maximum bank angle is reached, while in *Case 2* the maximum bank angle $\bar{\phi}$ is not reached.

The constants can be easily found from continuity conditions at $t = t_1$ and $t = \bar{t} - t_1$:

$$\begin{aligned} C_1 &= -\alpha\bar{u}\frac{t_1^2}{2} \\ C_2 &= -\alpha\frac{\bar{u}}{2}\left(2t_1^2 + \bar{t}^2 - 2\bar{t}t_1\right). \end{aligned}$$

At the end of the turn, $t = \bar{t}$, the heading angle is given by the following expression

$$\psi(\bar{t}) = -\alpha\bar{u}t_1^2 + \psi_0 + \alpha\bar{u}t_1\bar{t}. \quad (7)$$

*Case 2: The maximum bank angle is not reached.* In this case, the aircraft will initiate a maximum bank rate turn, and before the maximum bank angle is reached, it will start to come back to straight and level flight again. The bank angle for the entire turn can be written as

$$\phi(t) = \begin{cases} \bar{u}t, & t \in [0, \bar{t}/2] \\ -\bar{u}(t - \bar{t}), & t \in [\bar{t}/2, \bar{t}]. \end{cases} \quad (8)$$

The heading angle is then

$$\psi(t) = \begin{cases} \alpha\bar{u}\frac{t^2}{2} + \psi_0, & t \in [0, \bar{t}/2] \\ \alpha\bar{u}(t\bar{t} - \frac{t^2}{2}) + \psi_0 + C, & t \in [\bar{t}/2, \bar{t}]. \end{cases} \quad (9)$$

The constant $C$ can be easily found from the continuity condition at $t = \bar{t}/2$:

$$C = -\alpha\bar{u}\frac{\bar{t}^2}{4}.$$

The different cases are illustrated in Figure 1, where the time histories for bank angle and heading angle are shown for a *Case 1* and a *Case 2* turn.

## III. Path Planning

We present a simple path planning method to find candidate time-optimal paths between initial and final points in the plane. The motivation of the work is the optimality analysis presented in [13], as well as the

results presented in [14]. For simplicity of the discussion, we restrict our attention to those paths for which an initial turn is followed by a straight segment and a second turn. (The restriction requires that the the initial and final point are "sufficiently distant.") As in [10], we seek the solutions in terms of switching points, where the initial and final turns may be smoothly connected with a straight path. The point where the vehicle leaves the initial turn on the straight segment will be denoted as $P_A$, and the point where it starts the final turn will be denoted $P_B$. The path parameters at these points will be denoted as $t_A$ and $t_B$. Consider two paths in the plane, corresponding to the initial and final turns, and defined by the equations

$$x_1(t) = \int_0^t (V_a \cos\psi_1(\tau) + V_w)\, d\tau \quad (10)$$

$$y_1(t) = \int_0^t V_a \sin\psi_1(\tau) d\tau \quad (11)$$

$$x_2(t) = \int_0^t (V_a \cos\psi_2(\tau) + V_w)\, d\tau \quad (12)$$

$$y_2(t) = \int_0^t V_a \sin\psi_2(\tau) d\tau. \quad (13)$$

*Remark 3.1:* There is a slight abuse of notation here in using the same path parameter for the two paths.

The paths must satisfy the following conditions:

$$[x_1(0), y_1(0)]^T = [x_0, y_0]^T$$
$$[x_2(0), y_2(0)]^T = [x_f, y_f]^T.$$

Note that in this setting the second turn starts at path parameter $t = 0$, and the parameter value $t_B < 0$ corresponds to a configuration reached by integration in reverse time. With no bounds on the turn acceleration, equations (10)-(13) could be integrated to obtain closed-form expressions for the paths corresponding to trochoid curves [10]. The chief complication in the path planning problem presented in this paper is that there are no closed form solutions to the above integrals with the turn rate signals given in Section II. In the air-relative frame, the transition curves between straight segments and maximum turn rate segments are clothoid curves (Cornu spirals); the corresponding spatial coordinates $[x(t), y(t)]^T$ are special forms of the Fresnal-integrals [21], for which no analytical expressions exist. Consequently, the points $[x_1(t_A), y_1(t_A)]^T$ and $[x_2(t_B), y_2(t_B)]^T$ must be found by numerical integration.

Since the path connecting points $P_A$ and $P_B$ is a straight line, the heading angles have to satisfy the continuity equation:

$$\psi_1(t_A) = \psi_2(t_B) + 2k\pi, \quad k \in \mathbb{Z}, \quad (14)$$

where $\mathbb{Z}$ is the set of real integers.

Consider the following four types of trajectories. *Type 1* trajectories are those for which both the initial and final turns are *Case 1* turns, i.e. the maximum bank angle is reached. *Type 2* trajectories are those for which both the initial and final turns are *Case 2* turns, i.e. the maximum bank angle is *not* reached. *Type 3* (*Type 4*) trajectories are those for which the first (second) turn is *Case 1*, and the second (first) turn is *Case 2*. We present analysis results for *Type 1* and *Type 2* paths; the other two types can be computed in a similar fashion.

In both cases the objective is to find the straight path that connects points $P_A$ and $P_B$. At these two points the following additional continuity equations must be satisfied:

- The velocities at point $P_A$ and point $P_B$ must be equal:

$$(\dot{x}_1(t_A), \quad \dot{y}_1(t_A))^T = (\dot{x}_2(t_B), \quad \dot{y}_2(t_B))^T. \quad (15)$$

- The line segment joining points $P_A$ and $P_B$ must be tangent with the velocity vectors at both points:

$$\tan(\alpha) = \frac{y_2(t_B) - y_1(t_A)}{x_2(t_B) - x_1(t_A)} \quad (16)$$

$$\tan(\alpha) = \frac{\dot{y}_2(t_B)}{\dot{x}_2(t_B)} = \frac{\dot{y}_1(t_A)}{\dot{x}_1(t_A)}. \quad (17)$$

### A. Type 1 Extremals

In this case both the initial and final turns are *Case 1* turns. Substituting $\bar{t} = t_A$ into equation (7), we get the expression

$$\psi_1(t_A) = -\alpha\delta_1\bar{u}t_1^2 + \psi_{1_0} + \alpha\delta_1\bar{u}t_1 t_A,$$

where we have introduced the variable $\delta_1 \in \{-1, 1\}$ to denote the direction of the turn (left or right, respectively). Similarly,

$$\psi_2(t_B) = \alpha\delta_2\bar{u}t_1^2 + \psi_{2_0} + \alpha\delta_2\bar{u}t_1 t_B.$$

Notice that the sign of the terms has changed because of integration in reverse time, and because of the assumptions $t_1 > 0$ and $t_B < 0$. From the continuity equation (14), we get the expression

$$t_B = t_A\frac{\delta_1}{\delta_2} + \frac{\psi_{1_0} - \psi_{2_0}}{\alpha\delta_2\bar{u}t_1} - t_1\frac{\delta_1 + \delta_2}{\delta_2} + \frac{2k\pi}{\alpha\delta_2\bar{u}t_1}. \quad (18)$$

Using equations (15)-(17) one may obtain the following equation

$$\dot{y}_1(t_A)(x_2(t_B) - x_1(t_A)) = \dot{x}_1(t_A)(y_2(t_B) - y_1(t_A)).$$

Substituting equation (18) into the above expression, one obtains a single equation for $t_A$. This equation must be solved numerically. In this work, we use the bisection algorithm to obtain the root $t_A$. Once $t_A$ is known, $t_B$ may be found using equation (18).

### B. Type 2 Extremals

Substituting $t = t_A$ into equation (9), we get the expression

$$\psi_1(t_A) = \alpha\delta_1\bar{u}\frac{t_A^2}{4} + \psi_{1_0}.$$

Similarly,

$$\psi_2(t_B) = \alpha\delta_2\bar{u}\frac{t_B^2}{4} + \psi_{2_0}.$$

From the continuity equation (14), we get the expression

$$t_B = -\sqrt{\left|\frac{4(\psi_{1_0} - \psi_{2_0} + 2k\pi)}{\alpha\delta_2\bar{u}} + \frac{\delta_1}{\delta_2}t_A^2\right|}. \qquad (19)$$

As for Type 1 extremals, one may then obtain a single equation for the root $t_A$, which can be solved using the bisection algorithm, for example.

*Remark 3.2:* There are an infinite number of solutions for the above root-finding algorithm. These solutions correspond to those paths for which the air-relative velocity vector describes multiples of a full revolution before eventually joining the straight segment. Since those trochoidal segments for which the velocity vector describes more than two full revolutions cannot be optimal (see Lemma 3.2.2 in [20]), one can limit the number of possible solutions to a small set. Appropriately selected initial estimates for the root-finding algorithm will ensure that all roots in a given range are found. The minimum-time solution is selected among the candidates simply by comparing the total time required to complete each of the paths.

## IV. Results

The path planning method has been implemented for Type 1 and Type 2 trajectories. In the simulations, we used the parameter values $V_a = 20$ m/s, $V_w = 5$ m/s, $\bar{u} = 0.3$ rad/s, $\alpha = 0.4905$ 1/s, and $\bar{\phi} = 30°$.

Figure 2(a) shows the results of the path planning algorithm for a Type 1 path. The candidate time-optimal path is composed of a right turn followed by a straight path, then followed by a left turn. Both the initial and final turns are composed of three distinct segments: a maximum acceleration turn until the maximum bank angle is reached, a maximum bank angle segment, and a maximum acceleration turn bringing the aircraft back to straight and level flight. Figure 2(b) shows the time histories of the bank angle and the heading angle during the complete maneuver.

Similarly, Figure 3(a) shows an example where the candidate time-optimal path is a Type 2 trajectory. The turns are composed of segments where the maximum bank angle is not reached (see Figure 3(b)). Figure 4 shows all four candidate extremals. In this particular example all four extremals are Type 1 trajectories.

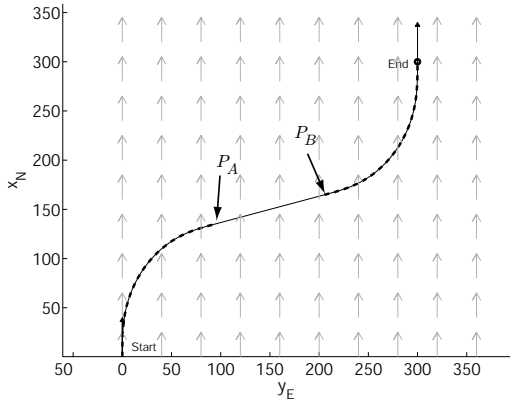


(a) Type 1 path.

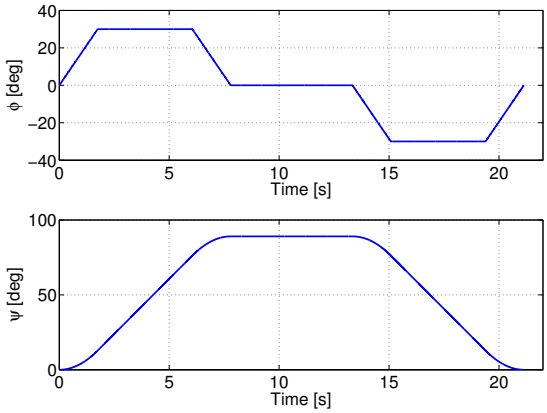


(b) Time histories of $\phi(t)$ and $\psi(t)$ for the above Type 1 maneuver.

Fig. 2. A Type 1 maneuver. In this case both the initial and final turns are saturated, i.e. the maximum bank angle is reached.

## V. Conclusions

This paper describes a path planning algorithm that generates candidate time-optimal paths between initial and final points in the horizontal plane with prescribed headings. The algorithm accounts for a steady, uniform ambient flow and accommodates bounds on turn rate and turn acceleration. Thus, the method generates smooth (continuous curvature) paths for flight vehicles that cannot change their turn rate instantaneously.

The method is immediately applicable for unmanned aerial vehicles flying in winds or for underwater vehicles in ocean currents. Our future work will focus on implementing the path-planning algorithm onboard underwater gliders and validating the paths' feasibility in experiments.


## Acknowledgements

The authors gratefully acknowledge the sponsorship of the Office Naval Research under Grants No. N00014-

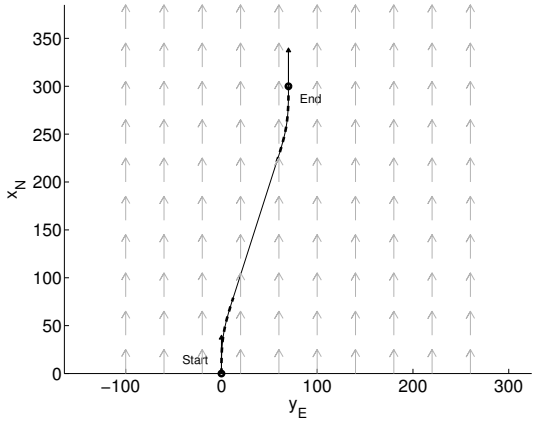


(a) Type 2 path.

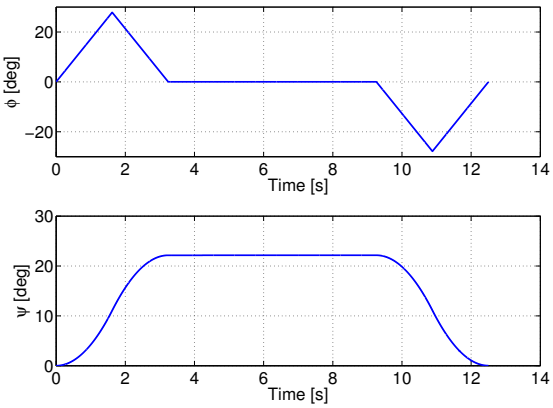


(b) Time histories of $\phi(t)$ and $\psi(t)$ for the above Type 2 maneuver.

Fig. 3. A Type 2 maneuver. Both the initial and final turns are completed without reaching the maximum bank angle.

08-1-0012 and No. N00014-10-1-0022.

## REFERENCES


[1] Bakambu, J. N. and Polotski, V., "Autonomous system for navigation and surveying in underground mines: Field Reports," *J. Field Robot.*, Vol. 24, No. 10, 2007, pp. 829–847.

[2] Murphy, R. R. and Stover, S., "Rescue Robots for Mudslides: A Descriptive Study of the 2005 La Conchita Mudslide Response," *J. Field Robot.*, Vol. 25, No. 1, 2008, pp. 3–16.

[3] Anon., "Unmanned Aircraft Systems Roadmap 2005-2030," Tech. rep., Department of Defense, August 2005.

[4] Dubins, L. E., "On curves of minimal length with a constraint on average curvature, and with prescribed initial and terminal positions and tangents." *American Journal of Mathematics*, Vol. 79, No. 3, 1957, pp. 497 – 516.

[5] Boissonat, J. D., Cerezo, A., and Leblond, J., "Shortest Paths of Bounded Curvature in the Plane," *Proc. of the IEEE International Conference on Robotics and Automation*, Nice, France, May 1992, pp. 2315 – 2320.

[6] Bui, X., Soukres, P., Boissonnat, J. D., and Laumond, J. P., "Shortest Path Synthesis for Dubins Non-holonomic Robot," *ICRA Technical Report*, INRIA, France, 1994.


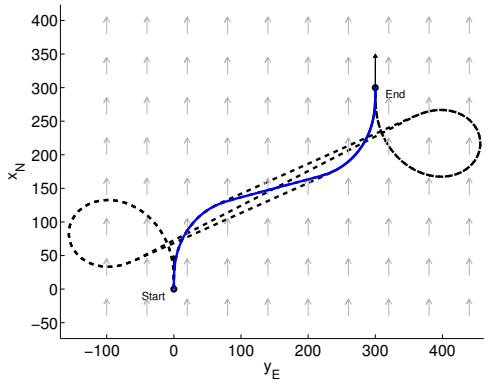


Fig. 4. Figure showing all four extremal paths. The candidate minimum-time trajectory is a Type 1 right turn followed by a straight line followed by a Type 1 left turn.


[7] McGee, T. G. and Hedrick, J. K., "Optimal Path Planning with a Kinematic Airplane Model," *Journal of Guidance, Control, and Dynamics*, Vol. 30, No. 2, 2007, pp. 629 – 633.

[8] McNeeley, R., Iyer, R. V., and Chandler, P., "Tour Planning for an Unmanned Air Vehicle under Wind Conditions," *Journal of Guidance, Control, and Dynamics*, Vol. 30, No. 5, 2007, pp. 1299 – 1306.

[9] Techy, L., Woolsey, C. A., and D. G. Schmale III, "Path Planning for Efficient UAV Coordination in Aerobiological Sampling Missions," *Proceedings of the 47th IEEE Conference on Decision and Control*, Cancun, Mexico, December 2008, pp. 2814 – 2819.

[10] Techy, L. and Woolsey, C. A., "Minimum-Time Path Planning for Unmanned Aerial Vehicles in Steady Uniform Winds," *Journal of Guidance, Control, and Dynamics*, Vol. 32, No. 6, 2009, pp. 1736–1746.

[11] Rysdyk, R. T., "Course and Heading Changes in Significant Wind," *Journal of Guidance Control and Dynamics*, Vol. 30, No. 4, 2007, pp. 1168 – 1171.

[12] Boissonnat, J. D., Cerezo, A., and Leblond, J., "A note on shortest paths in the plane subject to a constraint on the derivative of the curvature," *INRIA Technical Report*, No. 2160, INRIA, France, 1994.

[13] Kostov, V. and Degtiariova-Kostova, E., "Some properties of Clothoids," *INRIA Technical Report*, No. 2752, INRIA, France, 1995.

[14] Scheuer, A. and Fraichard, T., "Continuous-Curvature Path Planning for Car-Like Vehicles," *Proceedings of the IEEE International Conference on Intelligent Robots and Systems*, Grenoble, France, 1997, pp. 997 – 1003.

[15] Meek, D. S. and Walton, D. J., "Clothoid Spline Transition Spirals," *Mathematics of Computation*, Vol. 59, No. 199, 1992, pp. 117–133.

[16] Meek, D. S. and Walton, D. J., "A Note on Finding Clothoids," *Journal of Computational and Applied Mathematics*, Vol. 170, 2004, pp. 433–453.

[17] Meek, D. S. and Walton, D. J., "A Controlled Clothoid Spline," *Computers and Graphics*, Vol. 29, 2005, pp. 353–363.

[18] Hickerson, T. F., *Route Location and Design*, McGraw-Hill Book Company, New York, 1964, Chapter 6.

[19] Fleury, S., Soukres, P., Laumond, J. P., and Chatila, R., "Primitives for Smoothing Mobile Robot Trajectories," *IEEE Transactions on Robotics and Automation*, Vol. 11, No. 3, June 1995, pp. 441–448.

[20] Techy, L., *Flight Vehicle Control and Aerobiological Sampling Applications*, Ph.D. thesis, Virginia Tech, Blacksburg, VA, November 2009.

[21] Abramowitz, M. and Stegun, I. A., *Handbook of mathematical functions*, Dover, New York, 1965, page 300.